

Anisotropic diamagnetic response in type-II superconductors with gap and Fermi surface anisotropies

H. Adachi,^{1,*} P. Miranović,² M. Ichioka,¹ and K. Machida¹

¹ *Department of Physics, Okayama University, Okayama 700-8530, Japan*

² *Department of Physics, University of Montenegro, Podgorica 81000, Serbia and Montenegro*

(Dated: May 23, 2019)

Effects of anisotropic gap structures on a diamagnetic response are investigated in order to demonstrate that the field-angle-resolved magnetization ($M_L(\chi)$) measurement can be used as a spectroscopic method to detect gap structures. Our microscopic calculation based on the quasiclassical Eilenberger formalism reveals that $M_L(\chi)$ in a superconductor with four-fold gap displays a four-fold oscillation reflecting the gap and Fermi surface (FS) anisotropies, and the sign of this oscillation changes at a field between H_{c1} and H_{c2} . As a prototype of unconventional superconductors, magnetization data for borocarbides are also discussed.

PACS numbers: 74.25.Op, 74.25.Ha, 74.70.Dd

Precise determination of the node position or gap structure is of fundamental importance in superconductivity study in general, especially for ever-growing so-called unconventional superconductors since it is indispensable in identifying the pairing mechanism for a material of interest. There are only a few established methods for it; Angle-resolved specific heat and thermal conductivity measurements are notable ones^{1,2,3,4,5}. Nevertheless, to reinforce the conclusion, more such spectroscopic experiments based on bulk quantities are desirable⁶. As Takanaka⁷ suggested within the Ginzburg-Landau (GL) theory, a diamagnetic response is a strong candidate if combined with an analysis of the basal plane magnetization anisotropies. Needless to say a diamagnetic response from a superconductor is a hallmark of rigidity of the macroscopic wave function, containing a wealth of microscopic information, and it is a routine work to measure magnetizations to check if a material of interest is a superconductor or not. Since we are realizing⁵ that field-angle-dependences of various physical quantities such as specific heat or thermal conductivity should reflect low-lying quasi-particles around the vortex core, it is also expected that the magnetization contains the same kind of information.

Among a vast amount of type-II superconductors non-magnetic borocarbides RNi_2B_2C ($R=Lu,Y$) are considered to be typical examples of unconventional ones in the following sense: (i) Lots of experiments have demonstrated the existence of gap nodes (or gap minima)^{1,2,8,9,10}, (ii) the normal and mixed state properties behave well compared with other interesting materials such as cuprate superconductors, (iii) there exist detailed magnetization measurements^{11,12}. To establish a spectroscopic method based on the magnetization measurements it is thus important to understand the anisotropic diamagnetic response in these materials and clarify its relation to the gap structure.

In the works by Civale *et al.*¹¹ and Kogan *et al.*¹², basal plane magnetizations were measured as a function of the angle χ (see Fig. 1) between the applied field and the crystal axis, and it was found that the four-fold

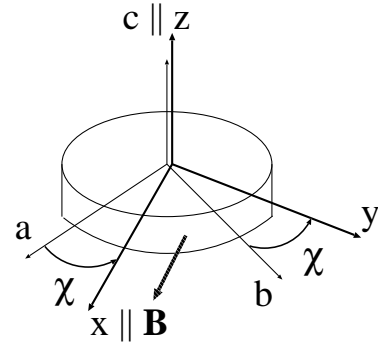


FIG. 1: The coordinates (x, y, z) and the crystal axes (a, b, c) . The induction \mathbf{B} is rotated from the a -axis by an angle χ .

oscillation of the magnetization showed a sign reversal with decreasing the field (or temperature). Kogan *et al.*¹² demonstrated that these behaviors can be reproduced within a nonlocal London theory without quoting anisotropy effects of the gap function. From a theoretical viewpoint it is quite reasonable to consider that the lower field (or lower temperature) behavior is well described within this framework since the London theory is believed to be appropriate for studying a vortex state in a field region $H \ll H_{c2}$. With increasing the field, however, the vortices start to overlap and the physics of vortex cores begins to play an essential role, whereas the core physics cannot be captured by any London theory without introducing some cutoff function by hand. As a consequence, at least when discussing anisotropy effects in a vortex state, the validity of London description in high fields is quite unclear. If we aim to clarify whether the observed phenomena are generic ones or not, we need a theoretical approach which can correctly describe the anisotropy of H_{c2} and the core effects.

The purpose of this letter is two-fold. The first one is to clarify the effects of gap structures on the anisotropic diamagnetic response based on the quasiclassical Eilenberger formalism. The second one is to apply our anal-

ysis to the prototype materials, i.e., nonmagnetic borocarbides, and present a microscopic description of the observed mysterious sign reversal of $M_L(\chi)$ -oscillation^{11,12}. Our microscopic treatment covers, of course, both GL theory and London theory, since the former is derived from the Eilenberger formalism through an expansion about the pair field, while the latter by using a phase only (London) approximation. Indeed our numerical solution at finite temperatures well reproduces both GL behavior ($M \propto H_{c2} - B$) near H_{c2} and London behavior ($M \propto \ln(H_{c2}/B)$) in lower fields.

Let us first explain our numerical procedure. We start with the following Eilenberger equation¹³ ($k_B = \hbar = 1$)

$$f(\varepsilon_n, \mathbf{p}, \mathbf{r}) = (2\varepsilon_n + \mathbf{iv} \cdot \mathbf{\Pi})^{-1} \left(2g(\varepsilon_n, \mathbf{p}, \mathbf{r}) w_{\mathbf{p}} \Delta(\mathbf{r}) \right), \quad (1)$$

where $g(\varepsilon_n, \mathbf{p}, \mathbf{r}) = \sqrt{1 - f(\varepsilon_n, \mathbf{p}, \mathbf{r}) f^\dagger(\varepsilon_n, \mathbf{p}, \mathbf{r})}$ and $f^\dagger(\varepsilon_n, \mathbf{p}, \mathbf{r}) = f^*(\varepsilon_n, -\mathbf{p}, \mathbf{r})$. Here $\varepsilon_n = 2\pi T(n + 1/2)$ is a fermionic Matsubara frequency, \mathbf{v} is a Fermi velocity, $w_{\mathbf{p}}$ is a orbital part of the gap function, $\mathbf{\Pi} = -i\nabla + (\Phi_0/2\pi)\mathbf{A}$ is a gauge invariant gradient, T_c is a transition temperature at a zero-field, and Φ_0 is the flux quantum. Throughout this paper the induction \mathbf{B} is directed along the x -axis (see Fig. 1). We treat extremely type-II superconductors with large GL parameter $\kappa \gg 1$ (in borocarbide superconductors $\kappa \gtrsim 10$), so that the vector potential is approximated by $\mathbf{A} = -Bz\hat{\mathbf{y}}$ where $\mathbf{B} = B\hat{\mathbf{x}}$. This is indeed a good approximation in high- κ case since the correction term is of order $O(1/\kappa^2)$. To solve Eq. (1), we adopt an approximation similar to that used by Pesch¹⁴,

$$f \approx 2gw_{\mathbf{p}}(2\varepsilon_n + \mathbf{iv} \cdot \mathbf{\Pi})^{-1} \Delta. \quad (2)$$

The physics behind this approximation is that the spatial variation of f related to the phase modulation of Δ is much larger than the spatial variation of g describing the amplitude fluctuation. It is worth noting that we do not replace g in the above equation by its spatial average as Pesch done, in order to ensure that the correct expression for the nonlocal GL free energy F/V given in Ref. 15 are reproduced up to the quartic term.

To proceed further with Eq. (2), it is convenient to expand the pair field into Landau levels,

$$\Delta = \Delta_0 \sum_{N=0}^{N_{\max}} d_N \psi_N, \quad (3)$$

$$\psi_N = \sum_{m=-\infty}^{\infty} C_m \frac{H_N(z + \nu m)}{\sqrt{2^N N!}} e^{-(z + \nu m)^2/2 - i\nu m y}, \quad (4)$$

where $\Delta_0 = 1.764T_c$, $r_B = \sqrt{\phi_0/2\pi B}$, $C_m = (\nu r_B/\sqrt{\pi})e^{-i\pi\zeta m^2}$, and H_N is the N -th Hermite polynomial. The real constants ζ and ν specify the configuration of a vortex lattice. Since the difference of a vortex lattice configuration is considered to be irrelevant to the quantity in question, we set in this paper $\zeta = 1/2$ and

$\nu = \sqrt{\sqrt{3}\pi}$; the value for a triangular lattice. Substituting the above expression into Eq. (2) and using a parameter representation

$$(2\varepsilon_n + \mathbf{iv} \cdot \mathbf{\Pi})^{-1} = \int_0^\infty d\rho e^{-(2\varepsilon_n + \mathbf{iv} \cdot \mathbf{\Pi})\rho}, \quad (5)$$

we have

$$f = 2gw_{\mathbf{p}} \int_0^\infty d\rho e^{-2\varepsilon_n \rho} \left(\Delta_0 \sum_{N=0}^{N_{\max}} \alpha_N d_N \right). \quad (6)$$

Here the expression for $\alpha_N \equiv e^{-i\rho \mathbf{v} \cdot \mathbf{\Pi}} \psi_N$ is given by

$$\alpha_N = \sum_m C_m \frac{H_N(z + \nu m - \text{Re } \lambda)}{\sqrt{2^N N!}} \times e^{-(|\lambda|^2 - \lambda^2)/4} e^{-(z + \nu m - \lambda)^2/2 - i\nu m y}, \quad (7)$$

where $\lambda = (v_z + iv_y)\rho/r_B$. At long last we have a solution for f , on condition that we have the correct $\{d_N\}$ -values. To determine $\{d_N\}$ we use the following selfconsistent equation projected onto each Landau level:

$$\left(\ln\left(\frac{T}{T_c}\right) + 2\pi T \sum_{n \geq 0} \varepsilon_n^{-1} \right) d_N = \frac{2\pi T}{\Delta_0} \sum_{n \geq 0} \overline{\psi_N^* \langle w_{\mathbf{p}}^* f \rangle}, \quad (8)$$

where the overbar denotes the spatial average, and the FS average $\langle \dots \rangle$ satisfies a normalization condition $\langle 1 \rangle = 1$; the definition is given by Eq. (11) below. Our numerical procedure is as follows: Input initial values for $\{d_N\}$, f , f^\dagger and g . Next use Eq. (6) to obtain the new f (and f^\dagger , g). Then iterate Eq. (8) to renew the $\{d_N\}$ -values, and return to Eq. (6). In order to check the reliability of our numerical procedure, we initially treated a two-dimensional case and calculated field dependences of each $\{d_N\}$ at $T/T_c = 0.5$. The obtained result was quite similar to the previous work based on the Landau level expansion of the GL equation (Figure 2(b) of Ref. 16). In the following calculation we use $N_{\max} = 6$.

The magnetization $4\pi\mathbf{M} = \mathbf{B} - \mathbf{H}$ is obtained from the relation $\mathbf{H} = 4\pi\nabla_{\mathbf{B}}(F/V)$. As for the longitudinal component $\mathbf{M}_L(\parallel \mathbf{H})$, which we focus on in this paper, Klein *et al.*¹⁷ obtained a more convenient formula extending the virial theorem derived by Doria *et al.*¹⁸:

$$-4\pi M_L = \frac{2\pi^2 N(0)}{B} T \sum_{n \geq 0} \left\langle \frac{2g(f^\dagger(w_{\mathbf{p}}\Delta) + f(w_{\mathbf{p}}\Delta)^*)}{1 + g} - 4\varepsilon_n \overline{(1 - g)} \right\rangle, \quad (9)$$

where in the above equation we approximately set $\mathbf{B} \cdot \mathbf{H} \simeq BH$ as in Ref. 12.

Now let us assume an isotropic FS to focus only on the role of the gap anisotropy. As a model for an anisotropic gap function, $w_{\mathbf{p}} = \sqrt{1 - \alpha \cos 4(\phi + \chi)}/\langle 1 - \alpha \cos 4(\phi + \chi) \rangle$ is used. Thus α denotes the degree of the gap anisotropy with $\alpha = 1$ being the nodal case. Figure 2

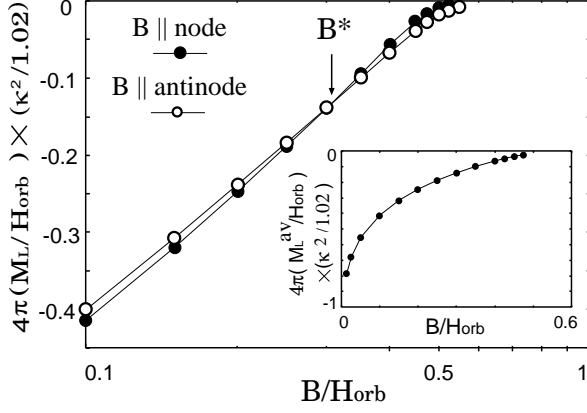


FIG. 2: Logarithmic field dependence of longitudinal magnetization M_L at $T/T_c = 0.6$ for $\mathbf{B} \parallel$ node (filled circles) and $\mathbf{B} \parallel$ antinode (open circles). The used anisotropy parameters are $\alpha = 1$ and $\beta = 0$. $H_{\text{orb}} = 1.037\Phi_0/2\pi\xi_0^2$ ($\xi_0 = v_0/2\pi T_c$) is the orbital limiting field in the isotropic case. Inset: Field dependence of $M_L^{\text{av}} = (M_L(\chi = 0) + M_L(\chi = \pi/4))/2$ for the same parameters.

shows the field dependence of the longitudinal magnetization M_L for $\mathbf{B} \parallel$ node (filled circles) and $\mathbf{B} \parallel$ antinode (open circles) at $T = 0.6T_c$. From the inset both the GL and the London behaviors are clearly seen. Although the difference of M_L between the two field-orientations is rather small, we can find that the M_L at $B \simeq H_{c2}$ is larger for $\mathbf{B} \parallel$ node, but with lowering the field this tendency is reversed at a field B^* . In Fig. 3(a), the corresponding field-angle dependences of $M_L(\chi)$ are plotted for several inductions. It should be emphasized here that the gap anisotropy *alone* can cause a sign reversal of the $M_L(\chi)$ -oscillation. The result with isotropic FS can be summarized as follows: $M_L^{B \parallel \text{node}} > M_L^{B \parallel \text{antinode}}$ in higher fields, and $M_L^{B \parallel \text{antinode}} > M_L^{B \parallel \text{node}}$ in lower fields.

Next we discuss the magnetization experiments^{11,12} for borocarbides. The observed data are incompatible with the above conclusion once we recall the experimental suggestion that the nodes exist along [100] and [010] directions^{1,2}. The discrepancy is considered to stem from the *unusually* large FS anisotropy possessing partial nesting¹⁹ in these materials. As a model having such an anisotropic FS, we introduce a four-fold anisotropic dispersion

$$\epsilon_{\mathbf{p}} = \frac{1}{2m} \left((p_x^2 + p_y^2)(1 + \beta \cos 4(\phi + \chi)) + p_z^2 \right) = \frac{p^2}{2m} \sigma^2, \quad (10)$$

where $\sigma(\theta, \phi) = \sqrt{1 + \beta \sin^2 \theta \cos 4(\phi + \chi)}$. Thus β denotes the degree of the FS anisotropy. The resultant Fermi momentum can be written as $\mathbf{p} = (mv_0/\sigma)\hat{r}$, where $\hat{r} = (\sin \theta \cos \phi, \sin \theta \sin \phi, \cos \theta)$ and v_0 is the Fermi velocity in the isotropic case. The Fermi velocity $\mathbf{v} = \nabla_{\mathbf{p}} \epsilon_{\mathbf{p}}$ can be expressed as $\mathbf{v} = v_r \hat{r} + v_\theta \hat{\theta} + v_\phi \hat{\phi}$, where $\hat{\theta} = (\cos \theta \cos \phi, \cos \theta \sin \phi, -\cos \theta)$ and $\hat{\phi} =$

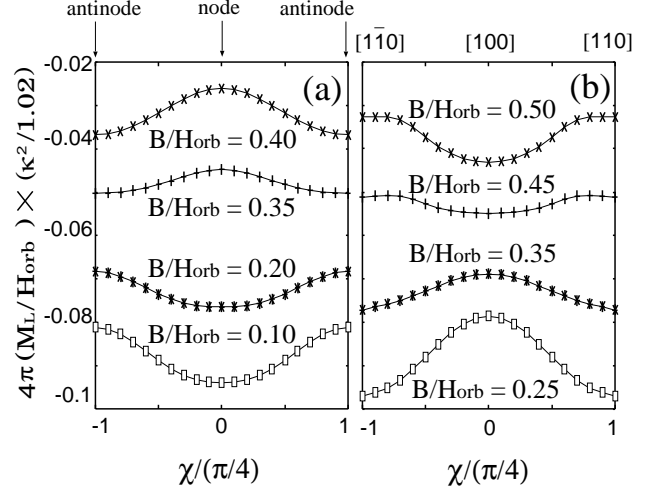


FIG. 3: Field-angle dependences of $M_L(\chi)$ for (a) $\alpha = 1, \beta = 0$ and (b) $\alpha = 1, \beta = 0.4$ at $T/T_c = 0.6$ for several inductions. The data at different B are vertically shifted.

$(-\sin \phi, \cos \phi, 0)$. Here each component of \mathbf{v} is given by $v_r = v_0 \sigma$, $v_\theta = 2v_0(\beta/\sigma) \sin^3 \theta \cos \theta \cos 4(\phi + \chi)$, and $v_\phi = -2v_0(\beta/\sigma) \sin^3 \theta \sin 4(\phi + \chi)$. Finally, the area element dS of the FS divided by $|\mathbf{v}|$ is given by $dS/|\mathbf{v}| = (m^2 v_0/\sigma^3) d(\cos \theta) d\phi$. Then our definition of the FS average is given by

$$\langle A_{\mathbf{p}} \rangle = \frac{\int_{\text{FS}} (dS \cdot A_{\mathbf{p}}/|\mathbf{v}|)}{\int_{\text{FS}} (dS/|\mathbf{v}|)}. \quad (11)$$

A band structure calculation for $\text{LuNi}_2\text{B}_2\text{C}$ suggests a rough estimate $\beta \simeq 0.4$ so as to reproduce the ratio $\langle v_a^4 \rangle / \langle v_b^2 v_c^2 \rangle = 0.128^{20}$ within our model.

Starting from the isotropic FS case ($\beta = 0$) and increasing the β -value, the oscillation pattern seen in Fig. 3(a) first tends to diminish, and when the β -value exceeds about 0.1, the sign of the $M_L(\chi)$ -oscillation pattern is completely reversed. This is shown in Fig. 3(b), and the oscillation behavior well coincides with the results of Refs. 11 and 12. It is worth noting that $\alpha\beta > 0$ in our model corresponds to the *competing anisotropy* case in the sense of Ref. 21, where the observed configuration²² of the vortex lattice in $\mathbf{B} \parallel c$ is properly explained by the competition between gap and FS anisotropies.

We show in Fig. 4 the field dependence of the magnetization oscillation amplitude $\delta M_L = M_L(\chi = \pi/4) - M_L(\chi = 0)$ at $T/T_c = 0.6$, which is to be compared with the experiments (Fig. 3 of Ref. 11 and Fig. 5 of Ref. 24). The characteristic behavior that δM_L is a slowly increasing function of the field except for a peak structure slightly below H_{c2} is well reproduced. Finally the inset of Fig. 4 shows the oscillation sign reversal field B^* in the B - T phase diagram for $\alpha = 1$ and $\beta = 0.4$. The $B^*(T)$ is a decreasing function of the temperature, and this is consistent with the experimental finding of Ref. 23. The $B^*(T)$ could be a diagnostic quantity to characterize the gap function and the FS anisotropy.

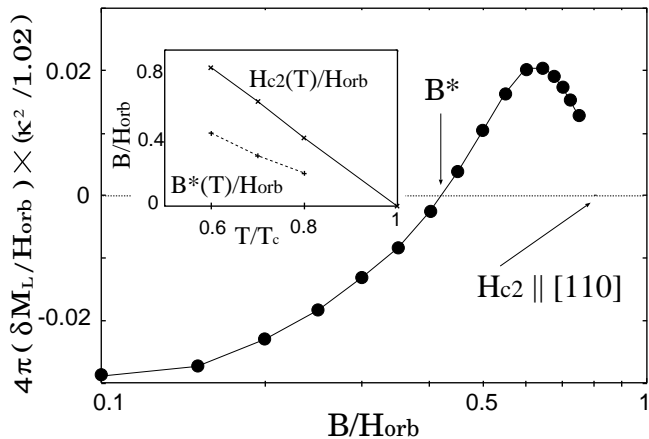


FIG. 4: Logarithmic field dependence of $\delta M_L = M_L(\chi = \pi/4) - M_L(\chi = 0)$ for $\alpha = 1, \beta = 0.4$ at $T/T_c = 0.6$. Inset: The sign reversal field B^* in the B - T phase diagram. The H_{c2} is determined through linear extrapolations of M_L .

The physics behind the phenomena is explained as follows: Near H_{c2} where the GL theory can be applied, the anisotropy of the longitudinal magnetization $4\pi M_L \simeq (B - H_{c2})/2.32\kappa^2$ comes from that of H_{c2} . In lower fields where the London theory is more appropriate, the anisotropy of $4\pi M_L \simeq (-\Phi_0/8\pi\lambda^2)\ln(H_{c2}/B)$ is *effectively* attributed to that of the penetration depth λ . Extending a knowledge on the relation between the ξ - and λ -anisotropies based on the anisotropic GL equation²⁵, a naive relation $H_{c2}(\chi = 0)/H_{c2}(\chi = \pi/4) \sim \lambda^2(\chi = 0)/\lambda^2(\chi = \pi/4)$ is expected to hold, where $\lambda(\chi)$ means an *effective* penetration depth *perpendicular* to $H_{c2}(\chi)$. Namely if H_{c2} is larger, then $1/\lambda^2$ is expected to be smaller, and this causes the sign reversal of the $M_L(\chi)$ -oscillation.

Before ending we briefly discuss the origin of the peculiar angular variation of $M_L(\chi)$ seen in Refs. 11 and 12. The low field $M_L(\chi)$ ^{11,12} have sharp maxima around [100] and [010] directions, and broader minima around [110] and $[1\bar{1}0]$ directions. The sharp maxima remind us of the observed cusp-like minima of thermal conductivity and specific heat^{1,2} around [100] and [010] directions. These have been argued as a result of so-called “s+g” pairing function¹. We calculated $M_L(\chi)$ for the pairing $w_{\mathbf{p}} \propto (1 - \sin^4\theta \cos 4(\phi + \chi))$ with point nodes keeping $\beta = 0.4$. However no such characteristic structure was observed in the angular dependence of $M_L(\chi)$. This means that explanations for the observed structure of $M_L(\chi)$ may need a different mechanism.

In conclusion we have microscopically studied field-angle-resolved basal plane magnetization oscillations, and demonstrated not only that a careful measurement of the magnetization can be a potentially useful tool to identify the nodal position of the gap function when a material of interest possesses less anisotropic FS, but also that the experimental data for borocarbides are well reproduced by considering both gap and FS anisotropies. If combined with other field-angle-resolved quantities²⁶, such as specific heat and thermal conductivity at low temperatures, we can further narrow down the possible pairing symmetry or gap anisotropy in various conventional and unconventional superconductors. The lesson from borocarbides tells us that for materials with unusually strong FS anisotropy such as borocarbides we should be careful to judge the nodal position through magnetization measurements, since unusually strong FS anisotropy can reverse the conclusion.

We would like to acknowledge useful discussions with T. Sakakibara and Y. Matsuda.

* adachi@mp.okayama-u.ac.jp

¹ K. Izawa, K. Kamata, Y. Nakajima, Y. Matsuda, T. Watanabe, M. Nohara, H. Takagi, P. Thalmeier, and K. Maki, Phys. Rev. Lett. **89**, 137006 (2002).
² T. Park, M. B. Salamon, E. M. Choi, H. J. Kim, and S.-I. Lee, Phys. Rev. Lett. **90**, 177001 (2003).
³ K. Izawa, H. Yamaguchi, Y. Matsuda, H. Shishido, R. Settai, and Y. Onuki, Phys. Rev. Lett. **87**, 057002 (2001).
⁴ H. Aoki, T. Sakakibara, H. Shishido, R. Settai, Y. Onuki, P. Miranović, and K. Machida, J. Phys.: Condens. Matter **16**, L13 (2004).
⁵ P. Miranović, N. Nakai, M. Ichioka, and K. Machida, Phys. Rev. B **68**, 052501 (2003).
⁶ There is an ongoing controversy on the gap function; either $d_{x^2-y^2}$ or d_{xy} pairings between angle-resolved thermal conductivity³ and specific heat⁴ experiments in CeCoIn₅.
⁷ K. Takanaka, J. Phys. Soc. Jpn. **65**, 3396 (1996).
⁸ M. Nohara, M. Isshiki, F. Sakai, and H. Takagi, J. Phys. Soc. Jpn. **68**, 1078 (1999).
⁹ T. Yokoya, T. Kiss, T. Watanabe, S. Shin, M. Nohara, H.

Takagi, and T. Oguchi, Phys. Rev. Lett. **85**, 4952 (2000).
¹⁰ I.-S. Yang, M. V. Klein, S. L. Cooper, P. C. Canfield, B. K. Cho, and S.-I. Lee, Phys. Rev. B **62**, 1291 (2000).
¹¹ L. Civale, A. V. Silhanek, J. R. Thompson, K. J. Song, C. V. Tomy, and D. McK. Paul, Phys. Rev. Lett. **83**, 3920 (1999).
¹² V. G. Kogan, S. L. Bud’ko, P. C. Canfield, and P. Miranović, Phys. Rev. B **60**, R12577 (1999).
¹³ G. Eilenberger, Z. Phys. **214**, 195 (1968).
¹⁴ W. Pesch, Z. Phys. B **21**, 263 (1975).
¹⁵ H. Adachi and R. Ikeda, Phys. Rev. B **68**, 184510 (2003).
¹⁶ T. Kita, J. Phys. Soc. Jpn. **67**, 2067 (1998).
¹⁷ U. Klein and B. Pöttinger, Phys. Rev. B **44**, 7704 (1991).
¹⁸ M. M. Doria, J. E. Gubernatis, and D. Rainer, Phys. Rev. B **39**, 9573 (1989).
¹⁹ S. B. Dugdale, M. A. Alam, I. Wilkinson, R. J. Hughes, I. R. Fisher, P. C. Canfield, T. Jarlborg, and G. Santi, Phys. Rev. Lett. **83**, 4824 (1999).
²⁰ V. G. Kogan, M. Bullock, B. Harmon, P. Miranovic, Lj. Dobrosavljević-Grujić, P. L. Gammel, and D. J. Bishop,

- Phys. Rev. B **55**, R8693 (1997).
- ²¹ N. Nakai, P. Miranović, M. Ichioka, and K. Machida, Phys. Rev. Lett. **89**, 237004 (2002).
- ²² M. R. Eskildsen, A. B. Abrahamsen, V. G. Kogan, P. L. Gammel, K. Mortensen, N. H. Andersen, and P. C. Canfield, Phys. Rev. Lett. **86**, 5148 (2001).
- ²³ L. Civale, A. V. Silhanek, J. R. Thompson, K. J. Song, C. V. Tomy, and D. McK. Paul, Physica C **341-348**, 1299 (2000).
- ²⁴ J. R. Thompson, A. V. Silhanek, L. Civale, K. J. Song, C. V. Tomy, and D. McK. Paul, Phys. Rev. B **64**, 024510 (2001).
- ²⁵ L. P. Gor'kov and T. K. Melik-Barkhudarov, Sov. Phys. JETP **18**, 1031 (1964).
- ²⁶ P. Miranović, M. Ichioka, N. Nakai, and K. Machida, cond-mat/0409371.